



The role of tidal forcing in the Gulf of Alaska's circulation

Guillermo Aoad¹ and Arthur J. Miller¹

Received 19 November 2007; revised 4 January 2008; accepted 14 January 2008; published 19 February 2008.

[1] High resolution (7 km) numerical simulations of the Gulf of Alaska circulation show an indirect effect induced by tidal forcing. Tides stir the water column more vigorously in the coastal ocean than in the Gulf's interior, leading to denser waters there than offshore. This horizontal gradient induces a geostrophic current that, in general and in most regions, flows against the mean general circulation. **Citation:** Aoad, G., and A. J. Miller (2008), The role of tidal forcing in the Gulf of Alaska's circulation, *Geophys. Res. Lett.*, 35, L04603, doi:10.1029/2007GL032727.

1. Introduction

[2] The sub-tidal circulation of the Gulf of Alaska (GOA) is characterized by coastal and near coastal currents along its eastern and western flanks [Stabeno *et al.*, 2004]. The Alaska Current, which runs northwestward along the northeast shelf-slope boundary, and the Alaska Stream, which runs southwestward parallel to the western shelf-slope boundary, both generate and feed the open-ocean with an energetic meso-scale circulation [Kelly *et al.*, 1993, Hermann *et al.*, 2002].

[3] The mean circulation of the GOA is unstable, especially on its eastern flank [Aoad, 1989]. The stability properties of the mean flow vary in time due in part to the structure, depth and sharpness of the thermocline. In turn, the latter is affected by buoyancy forcing, mean flow strength and ultimately by the overall effect of all forcing agents present in the region. The role of eddies in facilitating and leading the shelf-slope exchange of properties has been detailed by Okkonen *et al.* [2003]. They identified three different mechanisms by which eddies induce shelf-slope mixing of different physical and chemical properties.

[4] The GOA sea level exhibits one of the world's largest tidal amplitudes, especially for the dominant M2, S1 and K1 components. Stabeno *et al.* [2004] analyze the M2 component, reporting speeds of up to 70 cm/s at Kennedy Entrance and 30 cm/s at Gore Point and the Shelikof region. The sea level response to tidal forcing is maximum at the head of the GOA for the main semi-diurnal, M2, and diurnal, K1, harmonics [Foreman *et al.*, 2000]. Tidal mixing plays a leading role in cross-shelf exchange of properties in areas of strong across-shore topography gradients (e.g., canyons), a fact that carries important implications for the local biology [Ladd *et al.*, 2005].

2. ROMS Model

[5] The Regional Ocean Model System (ROMS) is an s-coordinate, terrain following, primitive equation model. It is

an optimized version of the SCRUM model [Song and Haidvogel, 1994], modified to run in multi-processor servers. This regional model has a horizontal resolution of 7 km, while in the vertical direction has 20 s-levels with increased resolution (~ 10 m) at the surface and (~ 300 m) near the bottom. This is achieved by setting a user-defined slow varying curve that determines the vertical resolution for each location. The interisland passes in the Aleutian Islands region are closed as our focus is farther upstream from this area. Two runs were carried out in order to assess the role of tidal forcing in the GOA. The only difference between these two runs was that one included tidal forcing while the other one did not. Other parameters and forcing functions remain identical between both runs. As required when using tidal forcing, Flather open boundary conditions were used for the barotropic flow [Flather, 1976], while zero gradient conditions were used for sea level.

[6] In this article, we term anomaly of a given variable to the difference between the values of the tidally forced run minus those from the run without tidal forcing. The initial conditions for the runs shown below were obtained after a 100-year long spin up run forced by NCEP [Kalnay *et al.*, 1996] climatological wind stresses and heat fluxes. The spin up run, in turn, was started from Levitus climatologies and rest showing no significant drift. Climatological open boundary conditions (OBC) were obtained from Levitus climatology while flow speeds were estimated assuming geostrophy. The tidal forcing enters the model through its open boundaries as both, sea surface height and tidal currents. The top 8-constituents (M2, K1, S2, K2, Q1, O1, N2, P1) were obtained from a global barotropic inverse tide model (TPX0.7) as described by Egbert and Erofeeva [2002]. Laplacian viscosity and diffusivity coefficients ($800 \text{ m}^2 \text{ s}^{-1}$ and $400 \text{ m}^2 \text{ s}^{-1}$, respectively) were only used in the model's sponge layers which are 50-km thick and are located all along the open boundaries. Those values only take place in the outer grid points of the sponge layers, exponentially decaying to zero towards the sponge layer's interior. NCEP [Kalnay *et al.*, 1996] climatological wind stresses and heat fluxes were also used, as in the spin up runs, to force our simulations. Even though we have not explicitly included freshwater forcing in our simulations, their climatological effect is implicitly present since both SSTs and SSSs are relaxed to their climatological values. However, temperature and salinity data (from the Levitus dataset) used to both relax SSTs and SSS, and to force the model through the open boundaries, contain residual tidal information which is small compared to the tidal cycle because monthly averages were used to drive (and relax) the model. Since both runs used identical initial conditions, relaxations, and surface and boundary forcing (aside from boundary tidal forcing), the tidal forcing effect can be properly isolated. The GOA's bottom topography is rich in canyons and banks while steep slopes, down to deep

¹Climate Research Division, Scripps Institution of Oceanography, University of California, San Diego, La Jolla, California, USA.

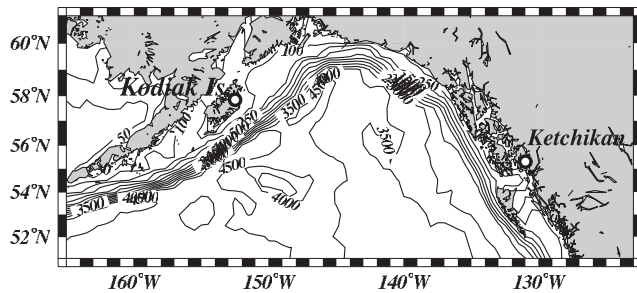


Figure 1. Bottom topography as isobaths. The two white circles denote the two locations where model sea level was contrasted against observations: Kodiak Island and Ketchikan City. Depths are in meters.

waters (~3000 m), characterize its margins (Figure 1). All these features have the potential of locally enhancing the tidal mixing effect through generation of vertical velocities due to sudden changes in the bottom depth. The Mellor-Yamada 2.5 closure scheme was selected to model vertical mixing in both runs. Our test results, comparing this scheme against others, confirm the findings of Robertson [2006] in that Mellor-Yamada 2.5 yields the most realistic results.

3. Results

[7] Tide gauge data from the COOPS program (noaa.gov) were used to validate our model results. Model sea level at

Kodiak and Ketchikan City stations (Figure 1) were compared against tide gauge observations (Figure 2) showing good agreement in amplitude and coherence. These were computed by extending the tidally forced run for an additional 15 days and saving sea level data every 30 minutes. This result suggests that our geographical domain is small enough to appropriately use lateral boundary tidal forcing.

[8] Climatological mean currents and mean sea level are shown in Figure 3 as annual averages. The main features of the GOA’s mean circulation are reproduced by the high-resolution model and these include the Alaskan Current, the Alaska Stream, the northern limb of the North Pacific current [Stabeno et al., 2004] and the eastward counter-current just south of the western end of the Alaskan Stream [Miller et al., 2005]. Mean flow speeds are in good agreement with those reported by Wu and Hsieh [1999] and Stabeno et al. [2004]. On the other hand, the anomalous flow field displays (Figure 3, right plot) a marked difference between the coastal (negative anomalies) and GOA’s interior (positive) sea level anomalies. Geostrophy dominates these anomalous fields since (i) surface anomalous currents tend to follow isolines of anomalous sea level (ii) areas of large anomalous sea level gradients coincide with areas of large anomalous velocities, and (iii) areas where the anomalous sea level gradient changes sign are accompanied by a change in the direction of the currents (e.g., some coastal areas, NE of Kodiak Island, the area around 142°W–60°N, etc). The eddy field (not shown) also showed good accord

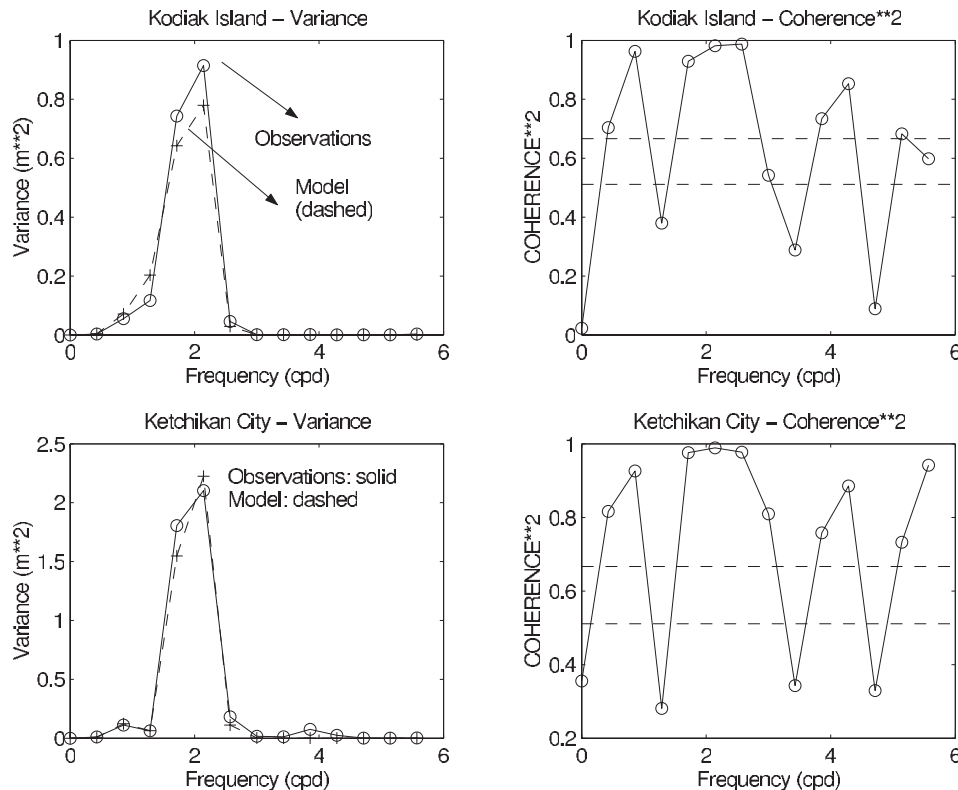


Figure 2. Cross spectral analysis contrasting the model’s sea level against tide-gauge observations for (top) Kodiak Island and (bottom) Ketchikan City, which locations are shown in Figure 1. The left plots show energy preserving variances vs. frequency, while the right plots display squared coherences vs. frequency. The two horizontal dashed lines on the right panels are the 90% and 95% confidence levels.

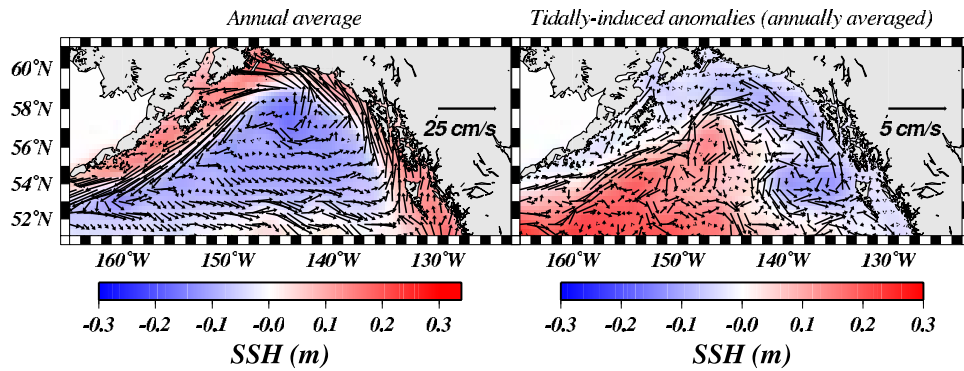


Figure 3. (left) Annually averaged sea level and surface currents for the tidally forced run. (right) Perturbations when we subtract the annually averaged tidally field from the unforced run from the one shown on the left (tidally forced).

with the descriptions given by *DiLorenzo et al.* [2006] and *Ladd et al.* [2007] for the Sitka and Haida eddies.

[9] The main effect of tidal forcing (Figure 4) is, not the most commonly reported tidal rectification process [*Loder, 1980*], but a mechanism that starts with increased top-to-bottom densities due to the action of active stirring. The intensity of this tidal mixing is naturally higher in coastal areas, and even larger where the bottom topography is rich in features that can induce a significant vertical mass transport. In the area located between 52°N–56°N and centered at about 137°W, fast residual flows are obtained (Figure 4, top right plot). This area combines unique features which can all potentially explain the complexities of the simulated residual currents seen in Figures 3 and 4.

Certainly, their combined effect is even more likely to generate distinctive flow patterns such as the one modeled here: a) the area overlaps with the bifurcation region of the North Pacific current. The residual flow pattern extends to same longitude, about 140°W, where the mean flow starts to bifurcate northward and southward, b) this is the only area in the GOA where a mean current, the North Pacific current, is normal to isobaths with fast decreasing depths, c) the main three tidal constituents, M2, K1 and S2, combine their maximum amplitudes (of the entire northeastern Pacific ocean) leading to one of the world regions with the highest mixing rates. In turn, this area of large mixing rates also leads to the characterization of another area, westward of it, where

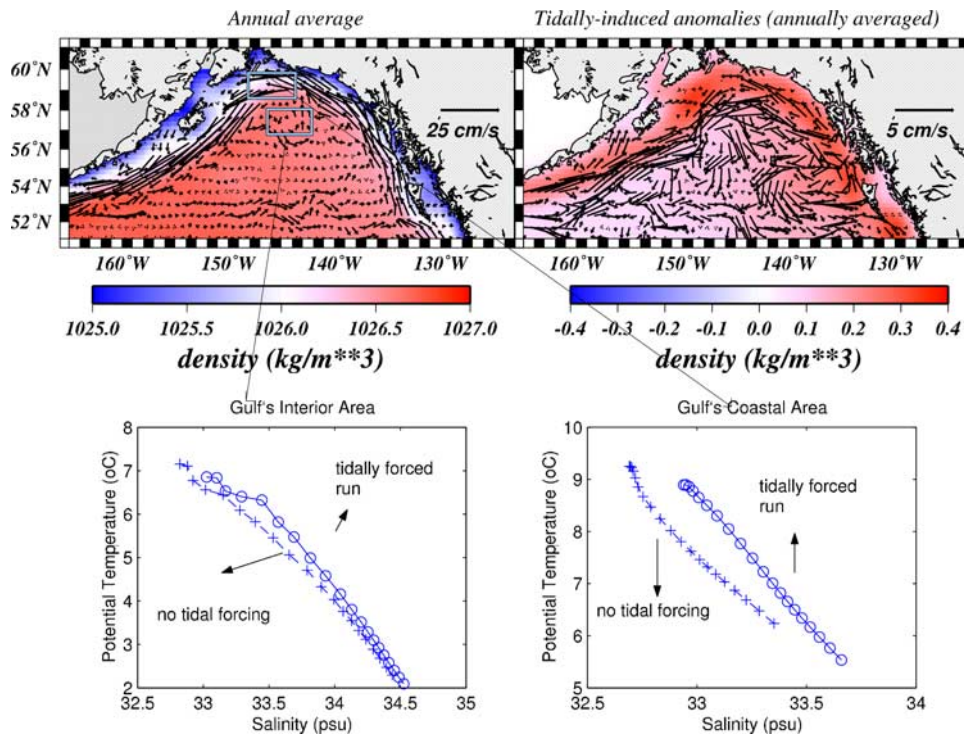


Figure 4. (left) Annually averaged density and currents at 80 m for the tidally forced run. (right) Perturbations when we subtract the annually averaged field from the tidally unforced run from the one shown on the left (tidally forced). The bottom plots show the spatially averaged T-S diagrams in the areas encompassed by the two rectangles shown on the top left plot: (bottom left) Gulf Interior's and (bottom right) Coastal. Note the higher mixing rates in the coastal ocean than in the Gulf's interior (for both areas) as well as the denser waters at all 20 levels for the tidally forced run.

sharp density gradients develop as a result of eastward-increasing mixing rates.

[10] A very similar chain of processes, i.e., differential tidal mixing generating density gradients and geostrophically driven currents, was recently reported in the northwestern Atlantic Ocean [Lee *et al.*, 2006]. The bottom plots in Figure 4 show how the model's density increased at all levels (top to bottom), and in both areas, after the inclusion of tidal forcing (solid line). The larger impact of tidal mixing in the coastal ocean than in the Gulf's interior, can be appreciated by comparing the separation between both lines in both plots. It is this gradient the one that drives the anomalous flow against the mean flow. Dynamic heights were computed for both runs and their difference estimated. These fields were consistent in both, phase and amplitude with the results shown above in Figures 3 and 4.

4. Conclusion

[11] The main effect of the tidal forcing in the GOA is to slow down the mean currents, through active tidal stirring, especially in areas of sharp topographic features (e.g., steep slopes). These near shore bottom-topography features amplify tidal mixing rates, as compared to the Gulf's interior, inducing horizontal density and sea level gradients which, in turn, drive anomalous geostrophic currents; the latter slow down the mean coastal circulation. If the current global warming is to persist, coastal waters will tend to become lighter due to both, increased runoff and increased SSTs. It remains to be studied how this scenario will evolve from current mixing rates. We speculate, since past warming events (e.g., 1976–1977 shift) have larger amplitude near the coast, and since runoff discharge takes place at the shoreline (leading to lighter waters), that the anomalous geostrophic currents described in this article will tend to decrease in amplitude in upcoming decades, thus contributing to accelerate the mean flows in the area. Targeted numerical experiments [e.g., Auad *et al.*, 2006] could certainly address this issue.

[12] **Acknowledgments.** Financial support was provided by the Department of Energy (FG02-04ER63857), by the National Science Foundation (OCE04-52692), by the National Oceanographic and Atmospheric Administration (NA17RJ1231) through the Environmental Climate Prediction Center (ECPC). This work was partially supported by the National Center for Supercomputing Applications under OCE060006N and utilized the NCSA Cobalt system. The views herein are those of the authors and do not necessarily reflect the views of NOAA or any of its sub agencies.

References

- Auad, G. (1989), Comments on "A quasi-geostrophic circulation model of the northeast Pacific. I: A preliminary numerical experiment," *J. Phys. Oceanogr.*, *19*, 1643s.
- Auad, G., A. Miller, and E. Di Lorenzo (2006), Long-term forecast of oceanic conditions off California and their biological implications, *J. Geophys. Res.*, *111*, C09008, doi:10.1029/2005JC003219.
- Di Lorenzo, E., W. Young, and L. Smith (2006), Numerical and analytical estimates of M2 tidal conversion at steep oceanic ridges, *J. Phys. Oceanogr.*, *36*, 1072–1084.
- Egbert, G., and S. Y. Erofeeva (2002), Efficient inverse modeling of barotropic tides, *J. Atmos. Oceanic Technol.*, *19*, 183–204.
- Flather, R. (1976), A model of the north-west European continental shelf, *Mem. Soc. R. Sci. Liege*, *6*, 141–164.
- Foreman, M. G. G., W. R. Crawford, J. Cherniawsky, R. F. Henry, and M. R. Tarbotton (2000), A high-resolution assimilating tidal model for the northeast Pacific Ocean, *J. Geophys. Res.*, *105*(C12), 28,629–28,651.
- Hermann, A. J., D. B. Haidvogel, E. L. Dobbins, and P. J. Stabeno (2002), Coupling global and regional circulation models in the coastal Gulf of Alaska, *Prog. Oceanogr.*, *53*, 335–367.
- Kalnay, E., et al. (1996), The NCEP/NCAR 40-year reanalysis project, *Bull. Am. Meteorol. Soc.*, *77*, 437–471.
- Kelly, K. A., M. J. Caruso, and J. A. Austin (1993), Wind forced variations in sea surface height in the northeast Pacific Ocean, *J. Phys. Oceanogr.*, *23*, 2392–2411.
- Ladd, C., P. Stabeno, and E. D. Cokelet (2005), A note on the cross-shelf exchange in the northern Gulf of Alaska, *Deep Sea Res., Part II*, *52*, 667–679.
- Ladd, C., C. Mordy, N. Kachel, and P. Stabeno (2007), Northern Gulf of Alaska eddies and associated anomalies, *Deep Sea Res., Part I*, *54*, 487–509.
- Lee, H.-C., A. Rosati, and M. J. Spelman (2006), Barotropic tidal mixing effects in a coupled climate model: Oceanic conditions in the North Atlantic, *Ocean Modell.*, *11*, 464–477.
- Loder, J. (1980), Topographic rectification of tidal currents on the sides of Georges Bank, *J. Phys. Oceanogr.*, *10*, 1399–1416.
- Miller, A. J., et al. (2005), Interdecadal changes in mesoscale eddy variance in the Gulf of Alaska circulation: Possible implications for the Steller sea lion decline, *Atmos. Ocean*, *43*, 231–240.
- Okkonen, S. R., T. J. Weingartner, S. L. Danielson, D. L. Musgrave, and G. M. Schmidt (2003), Satellite and hydrographic observations of eddy-induced shelf-slope exchange in the northwestern Gulf of Alaska, *J. Geophys. Res.*, *108*(C2), 3033, doi:10.1029/2002JC001342.
- Robertson, R. (2006), Modeling internal tides over Fieberling Guyot: Resolution, parameterization, performance, *Ocean Dyn.*, *56*, 430–444.
- Stabeno, P. J., N. A. Bond, A. J. Hermann, C. W. Mordy, and J. E. Overland (2004), Meteorology and oceanography of the Northern Gulf of Alaska, *Cont. Shelf Res.*, *24*, 859–897.
- Song, Y. T., and D. Haidvogel (1994), A semi-implicit primitive equation ocean circulation model using a generalized topography-following coordinate system, *J. Comput. Phys.*, *115*, 228–244.
- Wu, J. Q., and W. W. Hsieh (1999), A modelling study of the 1976 climate regime shift in the North Pacific Ocean, *Can. J. Fish. Aquat. Sci.*, *56*, 2450–2462.

G. Auad and A. J. Miller, Climate Research Division, Scripps Institution of Oceanography, University of California, San Diego, 9500 Gilman Drive, La Jolla, CA 92093, USA. (guillo@ucsd.edu)